RELIABILITY ANALYSIS OF WIND-SENSITIVE STRUCTURES

AHSAN KAREEM

Structural Aerodynamics and Ocean System Modeling Laboratory, Cullen College of Engineering, University of Houston, Houston, TX 77004 (U.S.A.)

Summary

The theoretical background of practical structural reliability methods encompassing numerical integration, approximate methods and simulation techniques is reviewed in the context of wind-excited structures. Their relative merits, shortcomings and limitations are addressed from the standpoint of their accuracy and computational efficiency. Quantitative reliability estimates of a concrete chimney are made, using different analysis procedures. Multiple potential failure modes are represented by the exceeding of the ultimate moment capacity at any level of the chimney height. The general bounds on the system failure probability are expressed in terms of the failure probability of the individual modes. The narrower bounds are established based on the existing theory by taking into account not only the failure probability of the individual modes, but also the joint failure probabilities in any two modes. Based on the findings of this study, it is suggested that the advanced first-order second-moment approximation and the simulation methods, which combine the Monte Carlo technique with variance reduction techniques, may provide accurate results for practical reliability analysis of wind-excited structures.

1. Introduction

Traditionally, structural safety in the design process is ensured by implementing appropriate safety factors to acknowledge shortcomings stemming from a lack of acknowledge, insufficient data or inherent variability in the problem parameters. The factor of safety concept does not provide a quantitative measure of the structural reliability. Even with the implementation of the safety factor, there exists a finite probability of failure of a structure. This is well recognized in the engineering community, but the concept of the safety factor is still widely accepted because of its simple nature and proven effectiveness for achieving safe design. The ensuring of structural safety by means of risk-consistent design requires assessment of uncertainties in the parameter space. This is followed by the propagation of uncertainties through the prescribed mathematical models of failure.

Probabilistic assessment of structural safety is receiving increased attention and acceptance with the emergence of probability-based design formats such

as the load and resistance factor design (LRFD) approach [1,2]. The review of reliability analysis techniques presented here, with a detailed example of wind effects on structures, is intended to stimulate more interest and to initiate further applications of reliability concepts in this field. It is envisaged that similar efforts will help to close the gap further between the state-of-the-art and the state-of-the-practice in probability-based design in wind engineering.

2. Theoretical background

Randomness and uncertainties associated with both wind loads and structural characteristics introduce variability in the dynamic response of wind-sensitive structures. The predicted response of structures based on mathematical and statistical models with imperfect knowledge tends to depart from reality. Recent developments in the area of probabilistic methods and statistical inference offer a mathematical basis that will enable designers to incorporate the influence of variabilities and uncertainties arising from a variety of sources more effectively into their design process. Some of these developments are discussed here from the standpoint of reliability of wind-sensitive structures.

2.1. Component reliability

The structural reliability analysis is accomplished by examining the limit states which describe the conditions that render a structure unsatisfactory for one of the intended roles under one load effect or a combination of load effects. From the ultimate strength standpoint, the limit state equation is generally expressed in terms of the structural resistance and load effects, whereas, for serviceability, the limit state represents the evaluation of a performance criterion, e.g., the exceeding of acceleration in tall buildings above a prescribed value. It is worth calling attention to the fact that it is often the serviceability limit state which governs the design of high-rise structures under winds.

The two basic variables representing action and resistance are functions of a number of other variables. An increase in the number of variables in the limit state equation and the departure of their distributions from the normal together with a nonlinear failure function introduces complexity to the problem. In this case, the limit state ($M=R-S=0$) is a hypersurface in n-dimensional space, and separates the failure and safe regions. The probability of failure is equal to the volume integral over the failure region

$$p_f = \int_{M(\mathbf{x})<0} f_{\mathbf{X}}(\mathbf{x}) \, d\mathbf{x} \tag{1}$$

in which $f_{\mathbf{X}}(\mathbf{x})$ is the joint probability density function of the n-dimensional vector $\mathbf{x}$. The preceding integral may be evaluated by means of one of the following techniques or a combination of them: (1) numerical integration, (2)

approximate methods, (3) simulation. In the following, a summary of these techniques is provided.

2.2. Numerical integration

The evaluation of the integral in eqn. (1) poses difficulties insofar as the description of the joint probability density of the system variables is generally not available. This is further compounded by the sizeable effort necessary to evaluate the integral involving a multiple numerical quadrature [3]. Approximations may be sought, but these are restricted to special cases of limited practical application [4]. Alternatively, a reduction in the multiplicity of the two- and three-dimensional integrations is possible by invoking the Stokes and Gauss divergence theorem [5].

2.3. Approximate methods

The approximate methods involve iterative algebraic techniques based on linearization of the limit state around an optimally chosen point. Linearization involves expansion of the limit state function into a Taylor series. By retaining the first-order terms, the failure surface is replaced with a hyperplane at the linearization point. This level of analysis is referred to as a first-order reliability analysis [5–9]. Generally, in practical situations, the information available on the resistance and load effects is only sufficient to estimate the first and second moments, i.e. the total uncertainty in each random variable is characterized by its mean and variance. This leads to the generally known first-order second-moment (FOSM) format. For better approximation, one must retain some higher-order terms in addition to the first two terms in the Taylor series expansion of the limit state function. The formulation which retains second-order terms is referred to as a second-order reliability analysis (SOR) procedure [5–13].

The FOSM approach in its simplest form involves linearization of the limit state surface at the mean values of the basic variables. Subsequently, the probability of failure may be expressed in terms of the uncertainties associated with the resistance and load effects. The first-order mean and variance of the limit state function M is given by

$$\bar{M} \approx M(\bar{x}_1, \bar{x}_2, ..., \bar{x}_n)$$

$$\sigma_M \approx \left[\sum_{i=1}^{n} \sum_{j=1}^{n} \left(\frac{\partial M}{\partial x_i} \right) \left(\frac{\partial M}{\partial x_j} \right) \mathrm{Cov}(x_i, x_j) \right]^{1/2} \tag{2}$$

The safety index or reliability index is expressed in terms of the mean and variances of the variables which appear in the limit state equation. If the variable M is assumed to be normal, the probability of failure p_f is given by

$$p_f = 1 - \Phi\left(\frac{\bar{M}}{\sigma_M}\right) = 1 - \Phi(\beta) \qquad (3)$$

in which $\Phi(\cdot)$ is the cumulative probability of the standard normal variate and β is the reliability index which is equal to M/σ_M. This approximation includes errors that stem from the presence of nonlinearity in the description of the limit state function with non-normally distributed variables. Furthermore, the linearization at the mean values fails to be invariant from equivalent limit states derived from different algebraic formulations. The FOSM formulation evaluated at the mean values of the basic variables is referred to as the MFOSM approach.

Alternatively, the limit state may be recast in terms of the reduced variables and linearized at the point on the failure surface closest to the origin, i.e. the point with the highest probability density. This point is generally referred to as the checking point or design point. This distance from the origin to the design point represents the reliability index β. This method is generally referred to as the advanced first-order second-moment (AFOSM) method, and it involves a search in the reduced transformed space for the point of maximum likelihood on the limit surface [5–9]. The correlated variables should be transformed to uncorrelated variables, for example, by means of the orthonormal eigenvectors of the covariance matrix [6,9]. The reliability index β is the solution to a nonlinear optimization problem with a given constraint. It can be calculated by using an iterative algorithm [5–11]. The algorithm may not converge in all problems and may not be able to distinguish between maxima, minima or saddle points. A different selection of starting points and careful evaluation of results may help to alleviate this shortcoming.

The probability of failure is approximated to first-order corresponding to the linearization of the failure surface, $p_f = \Phi(-\beta)$. The preceding concept may be further extended for problems with non-normal variables. For independent non-normal variables in the limit state equation, one possible choice involves transformation of the variables to equivalent normal variables [7–11]. For correlated non-normal variates, the Rosenblatt transformation is used [7–11].

Optimization procedures may be used in place of iterative techniques for the evaluation of β. In this context, determination of the minimum value of β may be cast as an optimization problem, where the distance from a point on the failure surface to the origin is minimized with the constraint that $M(X) = 0$. Any nonlinear programming technique may be used efficiently to solve this minimization problem [5]. An attractive feature of this approach is that the problem may be analyzed in the original coordinates, thus alleviating the need for the transformation to reduced variates. The advantage of analysis in the original space is fully realized for the limit states that are not explicitly defined.

The probability of failure derived from the reliability index gives a "reasonable" estimate of p_f for practical engineering problems. The p_f asymptotically is represented not only by the distance from the origin to the design point, but also depends on the principal curvature of the failure surface at the design points [12]. The size of the error introduced by linearization has been estimated for hyperspherical and parabolic limit surfaces in ref. 4. The difference between the exact and approximate solutions was found to be particularly distinct for an example case with small curvature and large dimensions.

As stated earlier, the first-order reliability methods may be improved by implementing the second-order reliability methods, in which the failure surface at the design points is approximated by a quadratic surface instead of a hyperplane. This approximation requires that the approximated quadratic and the actual failure surfaces at the design point have the same tangent hyperplane and second-order derivatives. It has been suggested [13] that in view of the other uncertainties in the analysis, the first-order reliability method may be sufficient for the analysis of practical problems.

2.4. Simulation methods

Simulation techniques offer the most versatile means of computing the probability of failure by using either the evaluation of the multiple-fold integration (eqn. (1)), or directly by simulating the failure phenomenon. Although the method may be used to solve virtually any reliability problem, the drawback is either in the statistical errors, or the cost of carrying out the necessary computations. The influence of the statistical uncertainties resulting from the use of only limited quantities of data to determine the statistical models and their parameters for simulation of the basic variables is inherent in the Monte Carlo simulation. For structures with very low probabilities of failure, a direct or a straightforward Monte Carlo simulation procedure may become computationally prohibitive. The Monte Carlo simulation technique may be made computationally more efficient by incorporating variance reduction techniques (VRT), e.g. conditional expectation, antithetic variates, importance sampling, correlated sampling, control variates, stratified sampling, latin hypercube sampling and a combination of VRTs [4,15–25]. For example, the simulation time can be reduced by limiting the simulated data in the tail part of the joint distribution of the basic variables. This leads to a dramatic reduction in the number of samples required, and the corresponding VRT is referred to as "importance sampling", which is briefly discussed later.

The direct Monte Carlo simulation involves simulation of the basic random variables according to their joint probability density function (JPDF). The number of points fallen within the domain, divided by the total number of points generated gives an estimate of the probability of failure in accordance with eqn. (1). The unbiased estimator of the probability of failure is given by

$$p_f = \frac{1}{N} \sum_{i=1}^{N} \delta_i \qquad (4)$$

in which $\delta_i = 0$, if $M(\mathbf{x}) > 0$, $\delta_i = 1$, if $M(\mathbf{x}) \leq 0$, and N is the total number of cycles.

The p_f obtained by means of Monte Carlo simulation is not "exact" as is generally true with any numerical solution. The previous equation provides the expected value of the probability of failure and the variance depends on the number of cycles. The number of simulations required to attain a prescribed level of confidence can be established.

The variance can be reduced by increasing the number of trials, but the number of cycles may not be increased beyond a certain limit because of the computational effort involved. If satisfactory results cannot be obtained with a reasonable number of trials, other means of reducing the error have to be sought. The VRTs, as pointed out previously, offer a means of reducing the variance of the simulated estimates of the failure probability without influencing its expected value. Detailed description and mathematical background is available [15], and applications of some of these techniques to reliability analysis have been addressed [4,15,21,23–25].

The unbiased estimate of the failure probability utilizing importance sampling is given by

$$p_f = \frac{1}{N} \sum_{i=1}^{N} \frac{\delta_i f_{\mathbf{X}}(\hat{\mathbf{v}}_i)}{h_{\mathbf{V}}(\hat{\mathbf{v}}_i)} \qquad (5)$$

in which $\hat{\mathbf{v}}_i$ is a vector of sample values taken from $h_{\mathbf{V}}()$ which is the "importance-sampling" probability density function and generally referred to as the sampling density. An optimal choice of the description of sampling density may reduce the variance of p_f to zero. Conversely, the variance of the estimator may actually increase because of a poor choice of the sampling density. One commonly used choice consists of using $f_{\mathbf{X}}(\mathbf{x})$ centered at the design points. In this manner, fewer points are required to estimate the probability of failure in comparison with the direct Monte Carlo simulation approach. The requirement of prior information on the design points often precludes the application of the importance sampling approach for problems on a single failure mode and lower nonlinearity in the failure surface. This is primarily a result of the suitability of the AFOSM approach in providing sufficiently accurate estimates of p_f once the design point is known.

In this study, conditional expectation, antithetic variates and a combination of these were used to improve the computational efficiency of the direct Monte Carlo simulation for estimating the probability of failure of a chimney under wind loading. The conditional expectation helps to reduce the order of integration in eqn. (1) and the variance of a simulated quantity by conditioning

on one or more of the basic variables appearing in the limit state equation with the least variance. The resulting conditional expectation is evaluated by a known theoretical expression. In this manner, only the variables with the least variance are simulated and the major source of random fluctuation is removed by not directly generating the associated variables. The antithetic variates approach involves introducing a negative correlation between the different simulation runs that leads to a reduction in the variation of the estimated quantity. By means of a pair of complementary random numbers for two cycles the desired negative correlation is conveniently introduced. Subsequently, a sample-mean of the simulated pair provides an explicit mathematical basis for variance reduction.

2.5. Alternative approximate methods

Before proceeding to the next section, it is worth commenting on other approximate methods available for the reliability analysis of wind-excited structures. Central to some of these methodologies is the approximation of the PDF of the limit state function or safety margin and hence the probability of failure. The simplest approach involves application of the Edgeworth series or Gram–Charlier series expansions [26]. A combination of the numerical integration and curve fitting using the Pearson family of frequency curves may be used for an approximate evaluation of the reliability. Higher-order moments in conjunction with multivariate Hermite series and polynomials have been shown to reflect accurately a wide range of nonlinear behavior that typifies distribution tails governing reliability [27,28].

Generally, a closed-form expression for the limit state function is available; however, for certain applications only an implicit description is possible. In such problems, a polynomial function fitted to the data obtained from, e.g. computer code runs may be used for the reliability analysis.

2.6. System reliability

The treatment of a structural system requires the analysis of various possible failure modes in which a system experiences loss of performance level either through its primary load-carrying role or deterioration resulting from excessive sway. Structural systems may be divided into two classifications, i.e. series and parallel systems. A series system fails to perform when any of its modes fail and survives only if all modes survive. A statically determinate structure performs like a series system. A parallel system fails only if all modes fail. The alternative load paths provide reserve resistance to the system against failure after the initial failure of any component. The behavior of a statically indeterminate structure is similar to a parallel system.

The exact evaluation of the reliability of a series system in terms of the failure probabilities in any mode, which are generally correlated, is not straightforward. Approximations are always sought. Several bounds on the

system probability of failure in terms of the individual failure modes and joint probabilities of failure in various modes have been suggested in the literature [e.g., 8,10,14,30,31]. Closer bounds are obtained if the joint probabilities of the failure in various modes are introduced. The analysis of a parallel system is more complicated and not as well developed as series systems, and is currently a subject of focused research. However, if the failure of a system is defined by the first failure of a component or a loss of serviceability at any location, the system may be treated as a series system. The example considered later in this paper belongs to a series system.

The probability of failure of a series system with n possible failure modes is given by the union of failure events $p_f = P[M_1 \cup M_2 \cup ... \cup M_n]$. The simplest bounds on the system failure probability may be expressed in terms of the failure probability of the individual modes

$$\underset{i=1}{\overset{n}{\text{Max}}} P[M_i] \leq p_f \leq \sum_{i=1}^{n} P[M_i] \tag{6}$$

Closer bounds on p_f have been formulated in terms of the failure probabilities in any mode and the joint failure probabilities in any two modes [14]

$$P[M_1] + \sum_{i=2}^{n} \max\left(0, P[M_i] - \sum_{j=1}^{i-1} P[M_i \cap M_j]\right)$$

$$\leq p_f \leq \sum_{i=1}^{n} P[M_i] - \sum_{i=2}^{n} \max_{j<i} (P[M_i \cap M_j]) \tag{7}$$

The individual modes and joint failure probabilities are approximated by

$$P[M_i] \cong \phi(-\beta_i)$$
$$P[M_i \cap M_j] \cong \Phi(-\beta_i, -\beta_j; \rho_{ij}) \tag{8}$$

in which ρ_{ij} represents the correlation between the linear safety margins and $\Phi(\,,;\rho)$ is the standard bivariate normal distribution.

The Monte Carlo simulation can be used to calculate system reliability. The system probability of failure is given by

$$p_{f(sys)} = \int_x \delta_x f_x(\mathbf{x}) d\mathbf{x} = \frac{1}{N} \sum_{i=1}^{N} \delta_x \tag{9}$$

in which δ_x is an indicator function that is equal to unity if $\underset{i=1}{\overset{n}{\cup}} M_i(\mathbf{x}) \leq 1$, otherwise zero, and $M_i(\mathbf{x}) = 0$ represents the ith limit state function and $\underset{i=1}{\overset{n}{\cup}} M_i(\mathbf{x})$ describes a union of n limit state functions. The importance sampling can be introduced to reduce the variance of the p_f estimator by directly extend-

ing the concept used in the single-failure mode (i.e. component reliability). In this case, the sampling density is derived from a weighted summation of a number of sampling subdensities of the respective failure modes. Further details on the application of importance sampling for system reliability may be found in refs. 4 and 29.

3. Example

Some of the concepts addressed in the preceding discussion on the reliability of structural components and systems will be illustrated in the following example of a wind-sensitive structure. This example will also shed light on the efficacy of some of the methods presented here from the standpoint of their relative advantages, disadvantages and accuracy.

A tall reinforced concrete chimney is used to illustrate the practical structural reliability techniques. The structural details of the chimney are given in ref. 32. Both the load effects and structural resistance parameters are treated as random variables. The limit states associated with the bending moment exceeding the moment capacity of the chimney cross-section at any level are considered.

The ultimate moment capacity of the chimney cross-sections at various heights was computed using a second-order stress–strain relationship for concrete [33]. The wind-induced load effects in both the along-wind and across-wind directions were formulated based on a covariance integration method [26,32,34]. The spectral description of the fluctuating wind load effects were used to predict the maximum bending moment associated with the different wind speeds by means of random-vibration-based techniques [26,32]. The predicted maximum values of the response were integrated with the meteorological statistics of the local climate.

The wind speed records for the site were analyzed to estimate the parameters of the annual extreme wind distribution. The selection of the extreme value distribution may be made based on Gumbel's classical method, or statistical inference using extreme-order statistics [35,36]. It should be emphasized that the extreme upper tail of the wind speed distribution may have a significant bearing on the estimation of the failure probability associated with very small risks. The available data on extreme winds are often very limited, which precludes validation of one distribution rather than another. The analysis of the tails of the distributions based on the extreme-order statistics offer alternative procedures to the traditional methods following the extreme-value distributions [36]. The generalized Pareto distribution is being considered for modelling the extreme events [36–38]. This approach facilitates reliable estimates based on limited data and also offers a possible upper limit to the magnitude of the extreme event. Currently, this approach is being used to model rainfall and variations in ocean wave height. Application to the prediction of

the extreme wind events is immediate and is a subject of current interest. For this study the extreme value Type I, Type II, and Rayleigh distributions were fitted to the data using the methods of moments and maximum likelihood. According to the maximum probability plot correlation coefficient (MPPCC) criterion, the Type I distribution was the most representative model of the wind records at the site [32,39].

The uncertainties in the parameter space were analyzed and their effect was propagated by means of the MFOSM approach to assess the structural reliability. A total of 25 basic variables were studied initially [26]. From a sensitivity analysis the number of variables was reduced to 13 for the present study. A description of the uncertainty analysis for the structural resistance and the load effects is omitted here for the sake of brevity; details may be found in refs. 26 and 32.

The lifetime failure probability of the example chimney is computed by means of MFOSM, AFOSM, direct Monte Carlo simulation and in conjunction with the variance reduction techniques. The procedures outlined earlier in the text are followed. A brief summary of the computational details involved in each technique is presented here to make this paper self-contained.

3.1. Mean value first-order second-moment method (MFOSM)

The coefficient of variation of the maximum lifetime structural response is expressed as [26,40]

$$\Omega_{(X_n^{(r)})_{\max}} = \frac{1}{(\bar{X}_n^{(r)})_{\max}} \left\{ \sigma_{(X_n^{(r)})_{\max}}^2 + \sum_{i=1}^{N} \left(\frac{\partial (x_n^{(r)})_{\max}}{\partial x_i} \bigg|_{\bar{x}_i} \right)^2 \Omega_{x_i}^2 \bar{x}_i^2 \right.$$

$$\left. + \sum\sum_{i \neq j} \rho_{x_i x_j} \frac{\partial (X_n^{(r)})_{\max}}{\partial x_i} \bigg|_{\bar{x}_i} \frac{\partial (X_n^{(r)})_{\max}}{\partial x_j} \bigg|_{\bar{x}_j} \Omega_{x_i} \Omega_{x_j} \bar{x}_i \bar{x}_j \right\}^{1/2}$$

$$(\bar{X}_n^{(r)})_{\max} = \left(\chi(\nu t_d) + \frac{\gamma}{\chi(\nu t_d)} \right) \sigma_{x_n^{(r)}}$$

$$\sigma_{(x_n^{(r)})_{\max}} = \left(\frac{\pi}{\sqrt{(6)}} \frac{\sigma_{x_n}^{(r)}}{\chi(\nu t_d)} \right) \tag{10}$$

in which $x_n^{(r)}$ represents a structural response component (e.g. moment at the nth node); γ is Euler's constant; $\chi(\nu t_d) = \sqrt{[2\ln(\nu t_d)]}$ and $\nu = 1/2\pi(\sigma_{x_n}^{(1)}/\sigma_{x_n}^{(0)})$; r represents higher derivations of response variable; and Ω represents the coefficient of variation of the subscript variable. The derivatives appearing in the preceding equation involve very lengthy expressions and have been omitted here for brevity [26]. The value of σ_{x_n} for $x_n^{(r)}$ representing moment is given by

$$\sigma^2_{M_n^{(r)}} = \left(\sum_{i=1}^{m} \phi^2_{ni} \left(\frac{\pi f_i \, S_{F_i}(f_i) \, 2\pi f_i)^{r-4}}{4 \, \xi_i \, M_i} \right) [T] \, [M] \{\phi_i\} \right)$$ (11)

in which $[T]$ and $[M]$ are the system transformation (which relates nodal forces to associated bending) and mass matrices and $S_{F_i}(f_i)$ is the model aerodynamic force spectrum. The maximum static and dynamic along-wind and across-wind load effects are combined, assuming independence of these load effects using the SRSS rule. However, in the case where any correlation exists among the load effects, appropriate inclusion of the correlation in a combination rule may result in a more realistic load combination. The uncertainty in the moment capacity representing resistance in combined axial loading and bending has been obtained on the basis of the FOSM approach and subsequently validated by Monte Carlo simulation [33].

The second-moment statistics of the limit state function or failure margin are derived from the statistics of the resistance and load effects, assuming statistical independence between them. The reliability indices and the associated probability of failure and their bounds are evaluated following the procedures outlined in the text.

3.2. Advanced first-order second-moment method (AFOSM)

The limit state equation is given by

$$M = m_R - (m_{\text{total}})_{\text{max}} = 0$$ (12)

In the previous equation m_R and $(m_{\text{total}})_{\text{max}}$ represent the ultimate moment capacity and maximum total applied load, respectively. As noted earlier, the expression for the total moments and the ultimate moment capacity are very lengthy, therefore, their documentation in this discussion is omitted [26]. The non-normal basic variables involved in these quantities are transformed to the equivalent normal variables as described earlier. This is followed by a search for the minimum value of β and associated probability of failure at each node. The bounds on the system probability of failure are computed, following the procedure described earlier [14].

3.3. Simulation techniques

3.3.1. Direct simulation

The basic variables appearing in the limit state function were simulated to match their prescribed probability distributions. The probability of failure was estimated by simulating directly the failure phenomenon (eqn. (10)).

3.3.2. Variance reduction techniques (VRTs)

3.3.2.1. *Conditional expectation.* Following the limit state function given in the previous section, the probability of failure is given by

$$p_f = P[M < 0] = P[m_{cw} > (m_u^2 - (m_{st} + m_{al})^2)^{1/2}] \tag{13}$$

in which m_{cw}, m_u, m_{st} and m_{al} represent the across-wind, ultimate, static and along-wind moments, respectively. The preceding equation may be recast into the form

$$p_f = P[m_{cw} > z|_{m_u, m_{st}, m_{al}}] \tag{14}$$

These equations reflect that the probability of failure is conditional on the parameters with lesser variability.

The probability of failure is simulated for N cycles and the mean and variance of the estimator of p_f is given by

$$\bar{p}_f = \sum_{i=1}^{N} p_{f_i}/N \qquad \text{var}(\bar{p}_f) = \frac{1}{N(N-1)} \sum_{i=1}^{N} (p_f - \bar{p}_f)^2 \tag{15}$$

3.3.2.2. *Antithetic variates.* In this technique a pair of separate simulation runs having a negative correlation are obtained for the failure probability. The average of the two runs provides an estimate of the mean failure probability

$$\bar{p}_f = \frac{1}{2N} \sum_{i=1}^{N} (p_{f_i}^{(1)} + p_{f_i}^{(2)}) \tag{16}$$

The variance of the failure probability is expressed as

$$\text{Var}(\bar{p}_f) = \frac{\text{Var}(\bar{p}_f^{(1)}) + \text{Var}(\bar{p}_f^{(2)}) + 2\text{Cov}(p_f^{(1)}, p_f^{(2)})}{4N} \tag{17}$$

It follows from the previous equation that the antithetic variate would be effective in reducing the variance if the covariance was strongly negative. This may be accomplished by using complementary random numbers to generate two runs in a pair, e.g. if U_k in a $U(0,1)$ random variable is used in the first run, then $1 - U_k$ is used in the second run to simulate the same variables. It is important for the success of the method to use the uniformly distributed numbers. The effectiveness in reducing variance of the simulated quantities may be impaired if other methods of generating random variables are used. The antithetic variates may be implemented in a simulation process in conjunction with other VRTs. In this study, the conditional expectation embedded with the antithetic scheme is used to compute the failure probability.

4. Results and discussion

The results of a deterministic analysis are presented in Table 1. The applied moments at various node levels are estimated from the distribution of wind pressure for which the chimney was designed (Fig. 1). The moments computed from the dynamic analysis using lifetime maximum wind at the site are also tabulated. The moment capacity at each level is used to compute the factor of safety against exceeding the ultimate moment capacity. These safety factors do not take into account any random variability in the parameters or modeling. The computed values of reliability index, β, obtained from the MFOSM and AFOSM are also reported in Table 1. Both the factors of safety and the reliability indices generally follow the same trend.

The results from the MFOSM, AFOSM, and simulation techniques are plotted in Figs. 2–5 for the mean value of the structural damping varying between 1 and 4%. These plots demonstrate that the results obtained from the MFOSM approach are much lower than those from the other methods. Because of the nonlinear nature of the failure surface and some of the basic variables being non-normal, the results of the MFOSM tend to be least reliable. The results from this approach should be interpreted cautiously unless the limit state function happens to be linear and the basic variables are normally distributed.

TABLE 1

Deterministic and probabilistic analysis

Node	Height (ft)	Diameter (ft)	Moment capacity (lb ft)	Wind-induced moment[a] (lb ft)	Factor of safety	Wind-induced moment[b] (lb ft)	Factor of safety	$\beta^{(1)}$	$\beta^{(2)}$
2	538	37.64	5.4485×10^7	2.3610×10^6	23	5.2806×10^6	10.3	6.13	2.81
3	478	39.45	7.5343×10^7	9.5720×10^6	7.9	1.9937×10^7	3.78	3.69	2.08
4	418	41.25	9.9183×10^7	2.1552×10^7	4.6	3.6023×10^7	2.75	2.99	1.91
5	358	43.06	1.2564×10^8	3.8434×10^7	3.27	5.3492×10^7	2.35	2.73	1.80
6	298	44.86	1.5498×10^8	6.0430×10^7	2.56	7.9735×10^7	1.94	2.08	1.57
7	238	46.67	1.8763×10^8	8.7758×10^7	2.13	1.1033×10^8	1.70	1.62	1.38
8	178	48.48	2.2803×10^8	1.2063×10^8	1.89	1.4507×10^8	1.57	1.38	1.25
9	118	50.28	2.9533×10^8	1.5926×10^8	1.85	1.8324×10^8	1.61	1.49	1.31
10	84	51.30	3.8166×10^8	1.8372×10^8	2.08	2.0645×10^8	1.85	1.98	1.53
11	54	52.21	4.2937×10^8	2.0651×10^8	2.08	2.2685×10^8	1.89	2.08	1.57
12	34	52.81	5.5886×10^8	2.2230×10^8	2.51	2.4261×10^8	2.31	2.80	1.81
13	14	53.41	4.7131×10^8	2.3858×10^8	1.98	2.5600×10^8	1.84	1.98	1.54
14	0	53.83	5.6815×10^8	2.5026×10^8	2.26	2.7402×10^8	2.07	2.38	1.69

[a]Code recommended values.
[b]Random vibration-based analysis.
$\beta^{(1)}$ – MFOSM.
$\beta^{(2)}$ – AFOSM.

508

PRESSURE DISTRIBUTION   LOAD DISTRIBUTION

98'

36 psf

400'

33 psf

100'

23 psf

598'

1290 #/ft
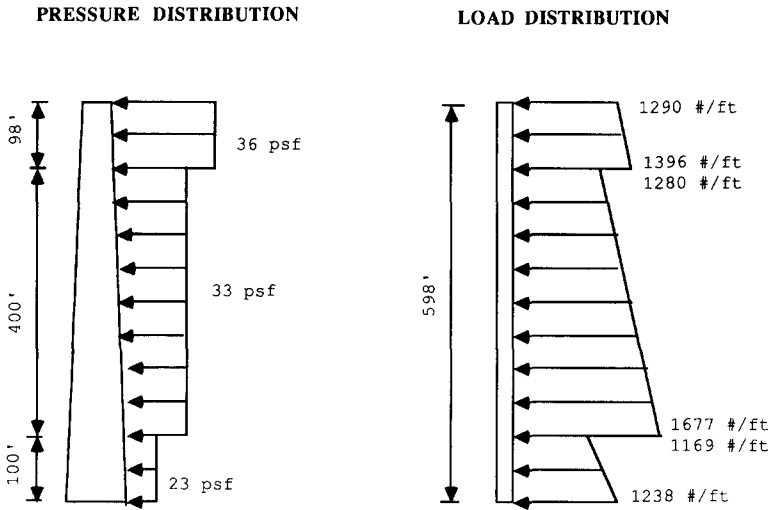
1396 #/ft
1280 #/ft

1677 #/ft
1169 #/ft

1238 #/ft

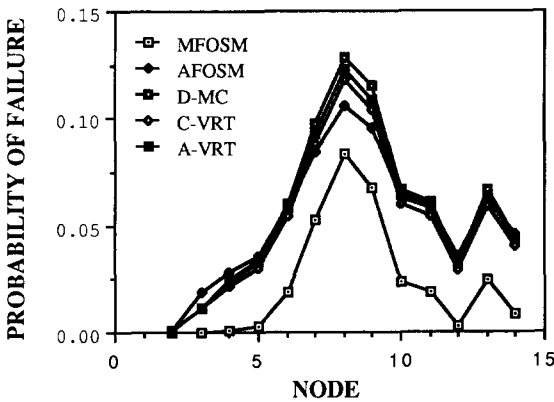Fig. 1. Pressure and load distribution on the chimney.

Fig. 2. Probability of failure at various nodes (damping ratio 1%).

The bounds on the probability of failure of the example problem were computed following the procedures discussed earlier. Simple bounds obtained by eqn. (6) are reported in Table 2 for different methods of analysis and damping values. The results reflect the trends observed in the failure probabilities of the individual modes. The narrower bounds given by eqn. (7) were computed for the MFOSM and AFOSM approaches by implementing the correlation between the various failure modes.

The narrower bounds on the failure probabilities computed on the basis of the correlations between the failure modes are also reported in Table 2. For the MFOSM approach, these bounds were only computed for the 1% damping case.
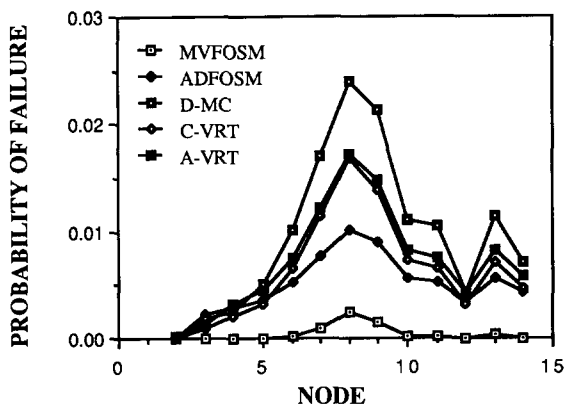
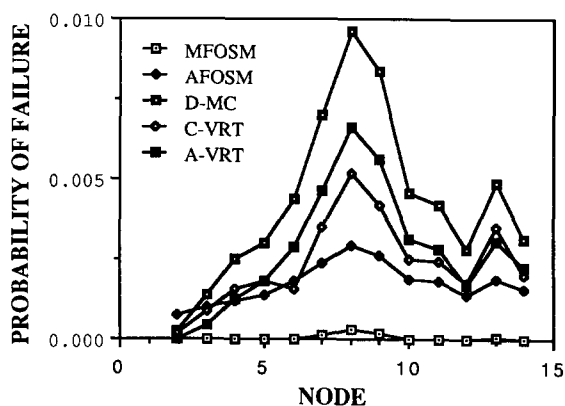Fig. 3. Probability of failure at various nodes (damping ratio 2%).

Fig. 4. Probability of failure at various nodes (damping ratio 3%).

The bounds for the AFOSM approach are sensitive to the ordering of the failure modes. The failure modes arranged according to the increasing value of the associated reliability indices provide a good choice of ordering [13]. It is noted that for the example problem the bounds obtained in this manner are almost coincident.

The sensitivity of the reliability index to the variations in the parameter-space, e.g. basic variables in the limit state equation or the parameters of their distributions, is often sought in reliability studies. For example, it permits the delineation of the parameters whose variability may have significant influence on the reliability index or the associated failure probability. It can be shown that the sensitivity of the reliability index to the variability in the basic variables is given by the numerical value of the corresponding direction cosines [8]. The sensitivity factors for the basic variables in the example problem
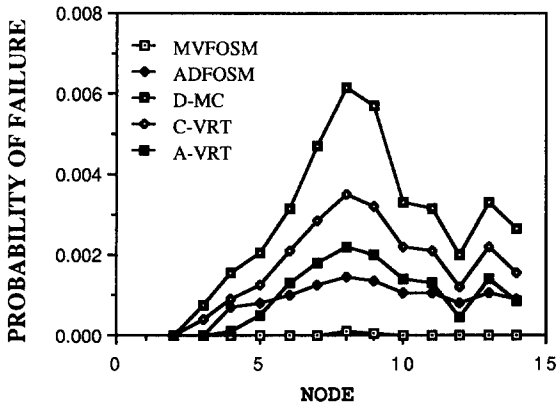
Fig. 5. Probability of failure at various nodes (damping ratio 4%).

TABLE 2

Bounds on lifetime probability of failure

Method damping	1%		2%		3%		4%	
	Lower	Upper	Lower	Upper	Lower	Upper	Lower	Upper
D-MC	0.1281	0.7411	0.0241	0.1264	0.0096	0.0545	0.00613	0.03853
C-VRT	0.1179	0.6723	0.0169	0.0838	0.0052	0.0310	0.00348	0.02339
A-VRT	0.1232	0.7137	0.0172	0.0952	0.0066	0.0362	0.00221	0.01331
AFOSM	0.1055	0.7111	0.0102	0.0650	0.0029	0.0200	0.00146	0.01141
AFOSM(N)	0.10553	0.10553	0.0102	0.0117	0.0029	0.0029	0.00146	0.00146
MFOSM	0.0833	0.3040	0.0024	0.0059	0.00029	0.00067	0.00018	0.00008
MFOSM(N)	0.09867	0.09922						

D-MC, Direct Monte Carlo; C-VRT, conditional VRT; A-VRT, antithetic VRT; AFOSM, advanced FOSM; MFOSM, mean-value FOSM; (N), narrow bounds.

together with the mean values, COVs and distributions are given in Table 3. It is noted that the reliability index is most sensitive to the structural and aerodynamic damping, and the parameters associated with the across-wind response, e.g. the Strouhal number and the lift or across-wind coefficient. This suggests that the across-wind response plays a significant role in the reliability of wind-excited chimneys. Omission of this component of response may have sizeable influence on the reliability estimates.

It should be noted that in this study the probability of failure is computed for the mean value of the damping ratio ranging from 1 to 4%. For the reinforced concrete structures, the damping value actually varies as a function of displacement. The analysis presented here can be extended to implement the variation of damping with amplitude in the evaluation of the load effects. How-

TABLE 3

Uncertainties of basic variables

Variable	Distribution	Mean	COV	α_i
B – Bandwidth of across-wind spectra	Lognormal	0.25	0.3	0.0822
C_D – Drag coefficient	Lognormal	0.7	0.14	0.0155
C_L – Across-wind force coefficient	Lognormal	0.15	0.27	0.4282
f – Natural frequency	Lognormal	—	0.17	0.0777
f_y – Steel yield stress	Lognormal	71 000 psi	0.093	−0.0892
f_c' – Concrete compressive stress	Normal	4000 psi/3390 psi 5000 psi/4028 psi	0.18 0.15	−0.00039
S – Strouhal number	Lognormal	0.20	0.11	−0.6122
ϵ_c – Concrete compressive strain	Normal	0.003	0.16	0.00924
ξ_a – Aerodynamic damping	Lognormal	—	0.30	0.4019
ξ_S – Structural damping	Lognormal	—	0.35	−0.4961
V – Wind speed, type I	Extreme value	52.91 mph	0.101	0.026
W – Weight of chimney	Normal	—	0.094	−0.1128

ever, a quantitative description of such a damping model for chimneys is not available, in part because of a lack of experimental data and complexity in the theoretical formulation. In the absence of such a damping description some empirical relationship may be used.

The procedures discussed in this paper can be applied in other areas of wind engineering design, e.g. serviceability of tall buildings, glass design, wind tunnel testing, low-rise structures and offshore structures. The software developed for this study is available on request. Additional examples on the reliability analysis of wind sensitive structures may be found in refs. 23 and 41–51.

5. Concluding remarks

Practical methods of reliability analysis of wind-excited structures, e.g. numerical, approximate and simulation techniques, are discussed. Their relative merits, shortcomings and limitations are highlighted from the standpoint of their accuracy and computational efficiency.

Although the numerical integration provides accurate results, its application is restricted to problems of low dimension, which are rarely of practical interest. The FOSM approximations offer a convenient practical solution to multidimensional problems. However, the applicability of the MFOSM is restricted to problem domains with linear limit state functions and normal basic variables. The AFOSM approach accounts for both the nonlinearity of the limit state functions and the non-normal basic variables. Although the second-order

reliability methods improve the first-order results, for most practical problems the first-order methods have been known to provide sufficiently accurate results. The straightforward simulation techniques suffer from the drawback of statistical errors or the prohibitive computational effort necessary for the large number of simulation cycles required to capture low failure probabilities. The direct simulation may be made computationally efficient by incorporating variance reduction techniques, e.g. conditional expectation, antithetic variates, importance sampling, stratified sampling and a combination of VRTs.

The application of the FOSM methods and simulation techniques together with VRTs in the reliability analysis are illustrated by means of an example of a tall reinforced concrete chimney exposed to wind loads. The results demonstrate that the advanced FOSM and the Monte Carlo simulation in conjunction with a VRT provide a good comparison of the failure probability. Based on the findings of this study, which involves a complex large-dimension problem, it is suggested that the advanced FOSM method and a combination of VRTs encapsulated within the Monte Carlo simulation may provide sufficiently accurate results for practical reliability analysis of wind-excited structures. The general and closer bounds on the failure probability of the example structure representing a series system are also evaluated.

Acknowledgements

References

1 B. Ellingwood and T.V. Galambos, Probability-based criteria for structural design, Struct. Safety, 1 (1982).
2 M.K. Ravindra and T.V. Galambos, Load and resistance factor design for steel, J. Struct. Div., ASCE, 104(ST9) (1978).
3 A.H. Stroud, Approximate Calculation of Multiple Integrals, Prentice-Hall, Englewood Cliffs, NJ, 1971.
4 G.I. Schueller and R. Stix, A critical appraisal of methods to determine failure probabilities, Struct. Safety, 4 (1987).
5 M. Shinozuka, Basic analysis of structural safety, J. Struct. Div., ASCE, 109(3) (1983).
6 A.H-S. Ang and W.H. Tang, Probability Concepts in Engineering Planning and Design, Vols. I and II, Wiley, New York, 1984.
7 G. Augusti, A. Baratta and F. Casciati, Probabilistic Methods in Structural Engineering, Chapman & Hall, New York, 1984.

8   H.O. Madsen, S. Krenk and N.C. Lind, Methods of Structural Safety, Prentice-Hall, Engle-
    wood Cliffs, NJ, 1986.

9   P. Thoft-Christensen and M.J. Baker, Structural Reliability Theory and Its Applications,
    Springer-Verlag, New York, 1982.

10 O. Ditlevsen and P. Bjerager, Methods of structural systems reliability, Struct. Safety, (3)
    (1986).

11 R. Rackwitz and B. Fiessler, Structural reliability under combined random load sequences,
    Comput. Struct., 9 (1978).

12 K. Breitung, Asymptotic approximation for multinormal domain and surface integrals, Sys-
    tem Modeling and Optimization, Proc. 11th IFIP Conf., Copenhagen, 1983.

13 H.O. Madsen, First order vs. second order reliability analysis of series structures, Struct.
    Safety, 2 (1985).

14 O. Ditlevsen, Narrow reliability bounds for structural systems, J. Struct. Mech., 7(4) (1979).

15 R.Y. Rubinstein, Simulation and Monte Carlo Method, Wiley, New York, 1981.

16 L.A. Twisdale, Analytic Monte Carlo: a new technique for the analysis of total uncertainty,
    Proc. ASCE Specialty Conf. Probabilistic Mechanics and Structural Reliability, Berkeley,
    CA, 1984.

17 J.M. Hammerseley and D.C. Handscomb, Monte Carlo Methods, Methuen, London, 1964.

18 A. Law and W. Kelton, Simulation, Modeling and Analysis, McGraw-Hill, New York, 1982.

19 A.W. Marshall, The use of multi-stage sampling schemes in Monte Carlo computations, in
    H.A. Meyer (editor), Symposium on Monte Carlo Methods, Wiley, New York, 1956.

20 J. Spanier, An analytic approach to variance reductions, SIAM J. Appl. Math., 18 (1970).

21 A. Harbitz, An efficient sampling method for probability of failure calculation, Struct. Safety,
    3 (1980).

22 J.E. Handschin, Monte Carlo techniques of prediction and filtering of nonlinear stochastic
    processes, Automatica, 6(3) (1970).

23 A. Kareem, Wei-Joe Sun and J. Hsieh, Reliability analysis of structures under dynamic wind
    loading, Proc. 5th U.S. Natl. Conf. Wind Engineering, Lubbock, TX, 1985.

24 B.M. Ayyub and A. Haldar, Practical structural reliability techniques, J. Struct. Eng., 110(8)
    (1984).

25 A. Kareem and J. Hsieh, Comparative study on methods of reliability analysis of concrete
    chimneys under winds, Proc. 4th Int. Conf. on Structural Reliability, Kobe, 1985.

26 A. Kareem and J. Hsieh, Reliability of concrete chimneys under winds, Department of Civil
    Engineering, University of Houston, Report UHCE 83-4, 1983.

27 M. Kohno and J. Sakamoto, Multivariate reliability analysis by Hermite polynomial approx-
    imation of non-normal distributions, in N.C. Lind (editor), Reliability and Risk Analysis in
    Civil Engineering, ICASP5, Vol. I, 1987.

28 S. Winterstein and P. Bjerager, The use of higher moments in reliability estimation, in N.C.
    Lind (editor), Reliability and Risk Analysis in Civil Engineering, ICASP5, Vol. I, 1987.

29 P. Bjerager, Probability integration by directional simulation, J. Eng. Mech., ASCE, 114(8)
    (1988).

30 C.A. Cornell, Bounds on the reliability of structural systems, J. Struct. Div., ASCE, 93(ST1)
    (1967).

31 E.H. Vanmarcke, Matrix formulation of reliability analysis and reliability based design, Com-
    put. Struct., 3 (1973).

32 A. Kareem and J. Hsieh, Reliability analysis of concrete chimneys under wind loading, J.
    Wind Eng. Ind. Aerodyn., 25 (1986).

33 A. Kareem and J. Hsieh, Statistical analysis of tubular reinforced concrete sections, J. Struct.
    Eng., ASCE, 114(ST4) (1988).

34 R.I. Basu and B.J. Vickery, Across-wind vibrations of structures of circular cross-sections,
    part II. Development of a mathematical model for full-scale applications, J. Wind Eng. Ind.
    Aerodyn., 12 (1983).

35   E.J. Gumbel, Statistics of Extremes, Columbia University Press, New York, 1958.
36   J. Pickands, Statistical inference using extreme order statistics, Ann. Statist., 3 (1975).
37   M.R. Leadbetter, G. Lindgren and H. Rootzen, Extreme and Related Properties of Random Sequences and Processes, Springer-Verlag, New York, 1983.
38   K.J.A. Revfeim and J.W.D. Hessell, More realistic distributions for extreme wind gusts, Q. J. R. Meteorol. Soc., 110 (1984).
39   E. Simiu and R.H. Scanlan, Wind Effects on Structures: An Introduction to Wind Engineering, Wiley, New York, 1986.
40   A.G. Davenport, The distribution of largest values of a random function with application to gust loading, Prog. Inst. Civ. Eng., London, 28 (1964).
41   A.G. Davenport, The relationship of reliability to wind loading, J. Wind Eng. Ind. Aerodyn., 13(1-3) (1983).
42   D.A. Reed, Glass cladding design for wind, Proc. 4th Int. Conf. on Structural Safety and Reliability, Kobe, 1985.
43   G.C. Hart, J.D. Ragett, S. Huang and S. Dow, Structural design using a wind tunnel test program and risk analysis, J. Wind Eng. Ind. Aerodyn., 14(1-3) (1983).
44   J.D. Holmes, Lam Pham and R.H. Leicester, Wind load estimation and safety index, Proc. 4th Int. Conf. Structural Safety and Reliability, Kobe, 1985.
45   K.B. Rojiani and Y-K. Wen, Reliability of steel buildings under winds, J. Struct. Div., ASCE, 107(ST1) (1981).
46   R.V. Milford, Structural reliability and cross-wind response of tall chimneys, Eng. Struct., 4 (1982).
47   L.A. Twisdale, Probability of facility damage from extreme wind effects, in J.M. Roesset (editor), Dynamics of Structures, Proc. Sessions at Structure Congress '87 Related to Dynamics of Structures, ASCE, New York, 1987.
48   G.I. Schueller, C.G. Bucher and P.H.W. Prenninger, Influence of mean wind speed, surface roughness and structural damping on the reliability of wind loaded buildings, Proc. 7th Int. Conf. Wind Engineering, Aachen, 1987.
49   E. Simiu and J.R. Shaver, Wind loading and reliability-based design in wind engineering, in J.E. Cermak (Editor), 5th Int. Conf. Wind Engineering, Fort Collins, CO, 1979, Vol. 2, Pergamon, New York, 1980.
50   Y-K. Wen, Wind direction and structural reliability II, J. Struct. Eng., ASCE, 110 (1984).
51   O. Ditlevsen, Fatigue model for elastic bars in turbulent wind, J. Wind Eng. Ind. Aerodyn., 18 (1985).